

## Supporting Information

### **Elucidating the Mechanism of Working SnO<sub>2</sub> Gas Sensors Using Combined Operando UV/Vis, Raman, and IR Spectroscopy**

*Ann-Kathrin Elger and Christian Hess\**

anie\_201908871\_sm\_miscellaneous\_information.pdf

# Supporting Information

## Table of Contents

### 1. Supplementary Material and Methods

1.1 Synthesis and Characterization

1.2 Gas Sensing

1.3 Spectroscopic Characterization

### 2. Supplementary Figures and Tables

Table S1: XPS data

Figure S1: *Operando* UV-Vis spectra

Figure S2: *Operando* Raman spectra

## 1. Supplementary Material and Methods

### 1.1 Synthesis and Characterization

For the gas sensing experiments commercial SnO<sub>2</sub> (Sigma Aldrich, 99.9% trace metals basis) was employed, which was calcined at 600°C (heating rate: 1.5°C/min) for 4 h before use. Based on N<sub>2</sub> adsorption experiments and application of the Brunauer–Emmett–Teller (BET) model, the specific surface area of the sample was determined as 7 m<sup>2</sup>/g. X-ray powder diffraction (XRD, STOE, STADIP, Cu<sub>Kα1</sub>-radiation,  $\lambda = 1.54060 \text{ \AA}$ , Ge[111] monochromator) revealed the presence of the cassiterite phase. Based on the Scherrer equation, the average crystallite size was estimated as 51 nm. The surface composition of the SnO<sub>2</sub> sample was studied by X-ray photoelectron spectroscopy (XPS, see Section 1.3).

### 1.2 Gas Sensing

For sensor preparation, the SnO<sub>2</sub> samples (~50 mg) were ultrasonically dispersed in deionized water and then dropwise placed on the surface of an Al<sub>2</sub>O<sub>3</sub>-transducer substrate with interdigitated Pt-electrodes (electrode distance ~150  $\mu\text{m}$ ) to measure the sheet resistance. On the other side of the substrate was a meander Pt-heater to heat the sensing material. The sensor was annealed at 85°C. The sample resistance was measured using a Keithley 175A Autoranging Multimeter. The temperature of the Pt-heater was calibrated prior to experiments. For gas-sensing experiments, the following gases (Westfalen AG) were used: oxygen 5.0 ( $\leq 0.2 \text{ ppm CO}_2, \leq 0.2 \text{ ppm C}_n \text{H}_m, \leq 3 \text{ ppm H}_2\text{O}, \leq 10 \text{ ppm N}_2 + \text{Ar}$ ), nitrogen 5.0 ( $\leq 3 \text{ ppm O}_2, \leq 1 \text{ ppm C}_n \text{H}_m, \leq 5 \text{ ppm H}_2\text{O}$ ), and 1000 ppm ethanol in nitrogen 5.0. The used carrier gas was synthetic air or nitrogen cycled with 250 ppm ethanol in synthetic air or nitrogen fed at 80 mL/min. Prior to all gas-sensing experiments the SnO<sub>2</sub> sample deposited on the substrate was calcined at 400°C in synthetic air for 30 min.

### 1.3 Spectroscopic Characterization

**X-Ray Photoelectron Spectroscopy.** X-ray photoelectron spectroscopy (XPS) was performed on a modified LHS/SPECS EA200 system using a Mg K $\alpha$  source (1253.6 eV, 168 W). XP spectra were recorded under UHV conditions. Calibration was done based on the Au 4f signal of gold foil at 84.0 eV and the Cu 2p signal of a copper plate at 932.7 eV.<sup>1</sup> Sample charging was accounted for by setting the C 1s position to 285 eV.

As shown in Table S1, XPS analysis of the commercial SnO<sub>2</sub> sample reveals the presence of Sn, O, and C at the surface. The Sn 3d photoemission confirms the presence of Sn<sup>4+</sup> without any indication of Sn<sup>2+</sup>. The O/Sn ratio was determined as 1.88, indicating a small oxygen deficiency at the surface as compared to the bulk. Based on C 1s detailed spectra, the presence of the carbon signal is attributed mainly to ubiquitous carbon as well as some carbonate.

**UV-Vis spectroscopy.** UV-Vis spectra were measured in diffuse reflection mode on an AvaSpec-ULS2048 (Avantes) using D<sub>2</sub> and halogen light sources. As the white standard, MgO powder was employed in the same geometry as the sample. The sampling time was 40 s, resulting from a 200 ms exposure time and averaging over 200 spectra.

**Raman Spectroscopy.** Raman spectra were collected in a 180° backscattering geometry using a 20 $\times$  objective (Olympus SLMPLN20x, WD: 25 mm, NA: 0.25). For excitation, we employed an Ar<sup>+</sup> laser (Melles Griot) operated at 514.5 nm. The applied laser power was 5 mW as measured with a power meter at the sample location (Ophir). As previously confirmed, at that power level and wavelength there was no damage on the sample even after several hours of laser irradiation. The backscattered light was dispersed using a HoloSpec *f*/1.8i Raman spectrometer (Kaiser Optical Systems) with an axial transmission grating and sent to a Peltier-cooled charge-coupled device (CCD) for detection. The resolution of the spectrometer is 5 cm<sup>-1</sup>; however, the wavelength stability was better than 0.5 cm<sup>-1</sup> as confirmed in a large number of

previous Raman spectroscopic studies on metal oxide materials such as ceria, see e.g. Refs. 2-5. Based on these the error bars are given as  $\pm 0.25 \text{ cm}^{-1}$ .

Raman spectra were collected continuously with an accumulation time of 800 s, including the application of a cosmic ray filter and subtraction of the dark spectrum (laser off). The *operando* cell used for all Raman experiments made no observable contribution to the Raman signal. Besides, gas-phase signals or signals of adsorbates on the  $\text{Al}_2\text{O}_3$  transducer substrate or the walls of the *operando* cell were not observed.

**Operando Spectroscopy.** A scheme of the experimental setup used for the *operando* experiments is shown in Figure 1. UV-Vis and Raman spectra were recorded in a custom-built *operando* cell. Products were analysed by FTIR spectroscopy (Bruker Vertex 70 FTIR spectrometer, pyroelectric DLaTGS (deuterated L-alanine doped triglycine sulfate) detector) in a small-volume (25 mL) gas cell (Axiom, LFT) heated to  $125^\circ\text{C}$  to avoid condensation. IR spectra were measured continuously with a resolution of  $4 \text{ cm}^{-1}$  and a measurement period of 300 scans ( $\sim 250 \text{ s}$ ) using the carrier gas as a reference. The IR gas-phase intensities of ethanol  $\text{CO}_2$ , and acetaldehyde were converted into concentrations using a set of calibration curves. To correlate the IR and gas-sensing measurements, the IR bands were baseline corrected and their concentrations were plotted against time. Any ethanol contribution was subtracted. As described previously,<sup>6</sup> the empty sensor substrate gave a negligible contribution at  $190^\circ\text{C}$ , and a measurable but insignificant contribution at  $325^\circ\text{C}$ .

Figure S1 depicts *operando* reflectance spectra (660–1000 nm) of the  $\text{SnO}_2$  gas sensor at  $325^\circ\text{C}$  in various gas environments. The spectra in Figure S1 correspond to the data set shown in Figure 1 (top panel), highlighting the region of higher wavelengths. As discussed in the context of Figure 1, the exposure to increasingly reducing gas environments ( $\text{air} \rightarrow \text{N}_2 \rightarrow \text{EtOH/air} \rightarrow \text{EtOH/N}_2$ ) results in a systematic decrease in the reflectance. The behaviour at higher wavelengths (660–1000 nm) strongly resembles the behaviour at 500–550 nm; however,

towards the NIR, a small decrease in the reflectance is observed, which may represent the onset of absorption by free charge carriers, which shows a wavelength dependence.<sup>7</sup>

Figure S2 shows *operando* Raman spectra (514.5 nm) of the SnO<sub>2</sub> gas sensor for two temperatures and various gas compositions. The spectra in Figure S2 correspond to the data set shown in Figure 1 (bottom panel), highlighting the region of low wavenumbers. The phonon region of the spectrum at 190°C in nitrogen is characterized by major Raman features at 473, 502, 544, 630, 690, and 770 cm<sup>-1</sup>. For comparison, at 325°C in nitrogen, the features appeared at 470, 501, 543, 626, 688, and 765 cm<sup>-1</sup>, in agreement with mode softening as a result of temperature induced lattice expansion. With 514.5 nm laser excitation, well-crystallized tin oxide has been reported in the literature to reveal characteristic Raman bands at 476 cm<sup>-1</sup> (E<sub>g</sub>), 629 cm<sup>-1</sup> (A<sub>1g</sub>), and 772 cm<sup>-1</sup> (B<sub>2g</sub>), besides additional features at around 500, 540, and 700 cm<sup>-1</sup>,<sup>8</sup> which is in very good agreement with Figure S2; the only noticeable difference is the intensity ratio of the 476 and 500 cm<sup>-1</sup> bands.

Under strongly reducing conditions, the *operando* Raman spectra reveal new bands at around 1350 cm<sup>-1</sup> and 1575 cm<sup>-1</sup>, which have been attributed to the D and G bands of carbon, respectively. As a result, other Raman features are strongly diminished or no longer detectable. Whereas the presence of the D and G bands is clearly evident in the spectrum recorded at 325°C in EtOH/N<sub>2</sub>, at 190°C in EtOH/N<sub>2</sub> only weak D and G bands are observed.

## 2. Supplementary Figures and Tables

**Table S1.** Surface composition of the SnO<sub>2</sub> sample based on the XPS analysis.

| Sample           | Sn / at% | O / at% | C / at% | O/Sn |
|------------------|----------|---------|---------|------|
| SnO <sub>2</sub> | 30.7     | 57.8    | 11.5    | 1.9  |

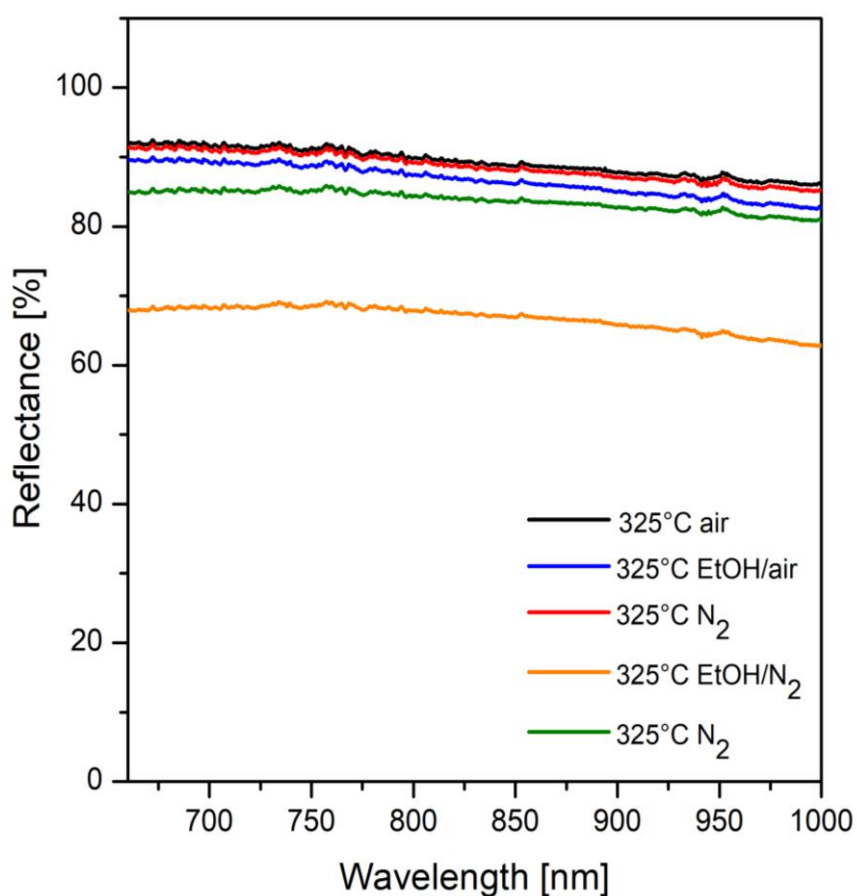


**Figure S1.** *Operando* reflectance spectra of the SnO<sub>2</sub> gas sensor at 325°C in various gas environments.

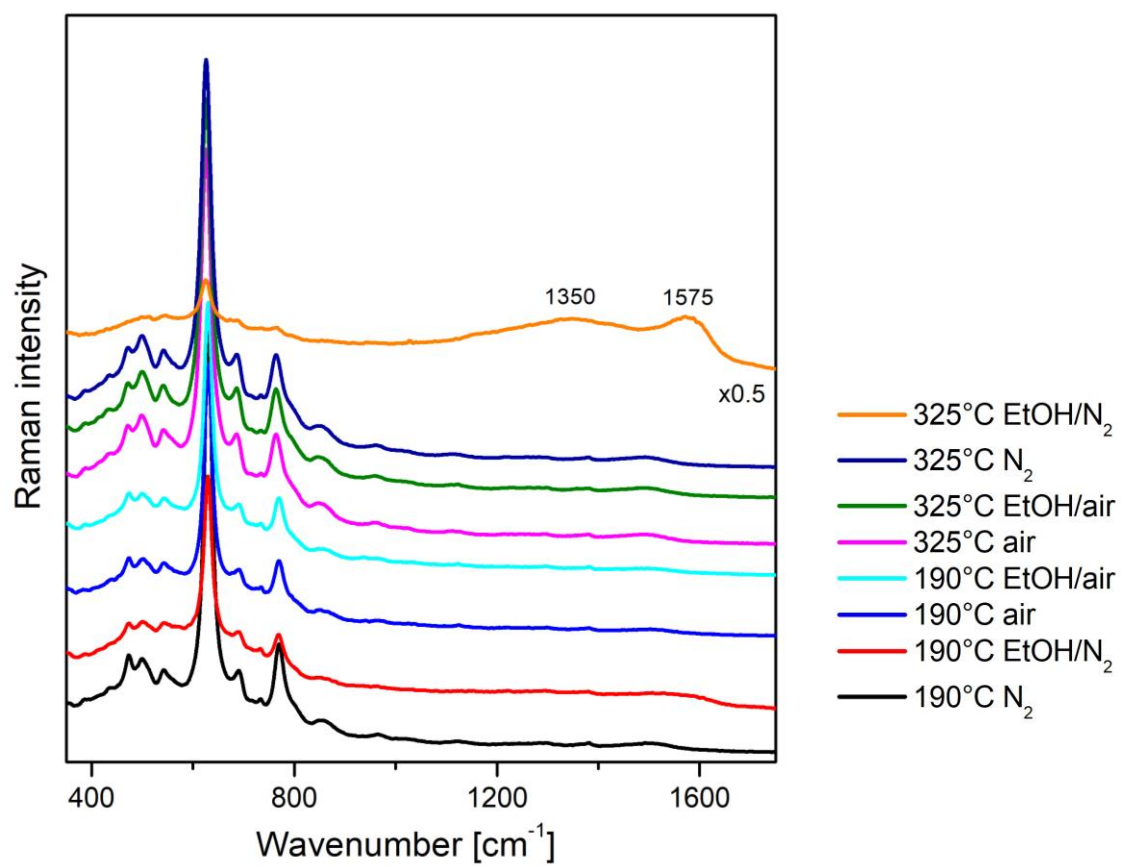


**Figure S2.** *Operando* Raman spectra of the SnO<sub>2</sub> gas sensor at two temperatures and various gas compositions recorded at 514.5 nm excitation. Spectra are offset for clarity.



## References

1. J. F. Moulder, W. F. Stickle, P. E. Sobol, K. D. Bomben, *Handbook of X-ray photoelectron spectroscopy*; Perkin Elmer, Eden Prairie, MN; 1992; Vol. 40.
2. C. Schilling, C. Hess, *J. Phys. Chem. C* **2018**, *122*, 2909-2917.
3. A. Filtschew, K. Hofmann, C. Hess, *J. Phys. Chem. C* **2016**, *120*, 6694-6703.
4. S. Sänze, C. Hess, *J. Phys. Chem. C* **2014**, *118*, 25603-25613.
5. A. Filtschew, C. Hess, *J. Phys. Chem. C* **2018**, *121*, 19280-19288.
6. S. Sänze, A. Gurlo, C. Hess, *Angew. Chem. Int. Ed.* **2013**, *52*, 3607-3610.
7. D. A. Popescu, J.-M. Herrmann, A. Ensuque, F. Bozon-Verduraz, *Phys. Chem. Chem. Phys.* **2001**, *3*, 2522-2530.
8. M. N. Rumyantseva, A. M. Gaskov, N. Rosman, T. Pagnier, J. R. Morante, *Chem. Mater.* **2005**, *17*, 893-901.